Acta Metallurgica, Vol. 27, pp. 1085 to 1095
Pergamon Press 1979. Printed in Great Britain

A MICROSCOPIC THEORY FOR ANTIPHASE BOUNDARY MOTION AND ITS APPLICATION TO ANTIPHASE DOMAIN COARSENING

SAMUEL M. ALLEN* and JOHN W. CAHN†

*Department of Materials Science and Engineering, Massachusetts Institute of Technology, Cambridge, MA 02139, U.S.A.
†Center for Materials Science, National Bureau of Standards, Washington, DC 20234, U.S.A.

(*Received* 12 *October* 1978)

Abstract—A microscopic diffusional theory for the motion of a curved antiphase boundary is presented. The interfacial velocity is found to be linearly proportional to the mean curvature of the boundary, but unlike earlier theories the constant of proportionality does not include the specific surface free energy, yet the diffusional dissipation of free energy is shown to be equal to the reduction in total boundary free energy. The theory is incorporated into a model for antiphase domain coarsening. Experimental measurements of domain coarsening kinetics in Fe–Al alloys were made over a temperature range where the specific surface free energy was varied by more than two orders of magnitude. The results are consistent with the theory; in particular, the domain coarsening kinetics do not have the temperature dependence of the specific surface free energy.

Résumé—Nous présentons une théorie microscopique de la diffusion appliquée au déplacement d'une paroi d'antiphase curviligne. Nous trouvons que la vitesse de l'interface est proportionnelle à la courbure moyenne du joint, mais, contrairement au cas des théories antérieures, la constante de proportionnalité n'inclut pas l'énergie libre superficielle spécifique, bien que la dissipation par diffusion de l'énergie libre soit égale à la diminution de l'énergie libre totale du joint. Nous incorporons cette théorie dans un modèle de la croissance des domaines antiphases. Nous avons effectué des mesures expérimentales de cinétiques de croissance des domaines dans des alliages Fe–Al, pour une gamme de températures dans laquelle l'énergie libre superficielle spécifique variait de plus de deux ordres de grandeur. Les résultats sont en bon accord avec la théorie; en particulier, les cinétiques de grossissement des domaines ne varient pas, en fonction de la température, comme l'énergie libre superficielle.

Zusammenfassung—Es wird eine mikroskopische, auf Diffusion aufbauende Theorie für die Bewegung einer gekrümmten Antiphasengrenze vorgelegt. Man findet, daß die Grenzflächengeschwindigkeit linear mit der mittleren Krümmung der Grenze zusammenhängt, die Proportionalitätskonstante jedoch anders als bei früheren Theorien die freie Oberflächenenergie nicht enthält. Es wird aber gezeigt, daß die durch Diffusion dissipierte freie Energie der Verminderung der gesamten freien Energie der Grenze entspricht. Die Theorie wird in ein Modell der Vergröberung von Antiphasendomänen eingearbeitet. Die Kinetik der Domänenvergröberung wird an Fe–Al-Legierungen experimentell über einen Temperaturbereich gemessen, in dem die spezifische freie Oberflächenenergie über mehr als zwei Größenordnungen variiert. Die Ergebnisse stimmen mit der Theorie überein; insbesondere weist die Kinetik der Domänenvergröberung die Temperaturabhängigkeit der spezifischen Oberflächenenergie nicht auf.

1. INTRODUCTION

Internal surfaces in solids—such as grain boundaries, coherent interphase interfaces and antiphase boundaries—are in general non-equilibrium features of real crystalline solids. They have a positive excess free energy. Thus, in polycrystalline materials, grain boundaries migrate to reduce the total amount of grain boundary area. Local atomic arrangements near rapidly moving interfaces can differ significantly from arrangements near slowly moving ones, giving rise, for example, to impurity-drag phenomena. A complete theory of interfacial motion in solids would have to account not only for the local structure, excess free energy and geometry of the interface, but also for the topological nature of the interfaces as a whole, in order that the evolution of the microstructure could be understood.

Resistances to interfacial motion in solids are often diffusional. Grain growth in pure metals requires rearrangement of atoms in a grain boundary region, thus requiring diffusion over distances of the order of an atomic spacing. Long-range diffusion can also be required for interfacial motion, such as for the growth of a precipitate from supersaturated solution, or in cases where impurities segregate to the interface and tend to be carried along with the interface as it moves.

Theories to explain many of these phenomena have been proposed [1–4]. A widely-used phenomenological theory of interfacial motion [1, 2] states that inter-

facial velocity V is proportional to thermodynamic driving force, the proportionality constant being a positive quantity called the mobility. The driving force in this theory is the product of the mean of the local principal curvatures $(K_1 + K_2)$ of the boundary and its excess free energy per unit area σ, resulting in the relationship

$$V = \mu\sigma(K_1 + K_2), \tag{1}$$

where μ is the mobility which in some theories is inversely proportional to interface thickness [2]. One of the motivations for the present study was to test equation (1) experimentally for a problem in which the surface free energy dependence could be investigated. When an order–disorder transition is higher-order, the antiphase boundary (APB) energy is known to tend to zero continuously at the transition temperature [5], thus providing a means to vary the magnitude of the surface free energy over a wide range.

Another approach to the theory of interfacial motion, used by Langer and Sekerka [6], is based on solving a diffusion equation that has been modified to account for the thermodynamics of non-uniform systems [7]. The premise is that this modified free energy is the basis of a diffusion potential whose gradient leads to a flux [8]. Langer and Sekerka have used this diffusion theory to describe motion and deviations from equilibrium in a plane interface between two phases differing in composition and being forced to move because of imposed fluxes through the bulk phases. The mathematical problem was quite cumbersome in that there were three regions with differing diffusion scales: the two phases and the interfacial region itself. Interfacial motion was controlled by long-range diffusion.

A much easier problem to study using the diffusion-theory approach is the motion of a curved APB. These are coherent interfaces separating domains with identical properties in crystals with long-range order, the domains differing by a relative displacement which is not a superlattice translation. If the differences between the atomic species were ignored, the two domains would be part of the same crystal.

There are alternative ways of considering APBs and their properties. It is customary to think of them as surfaces, having geometrical properties such as area and curvature, thermodynamic and chemical properties such as excess free energy per unit area and adsorption, and kinetic properties such as their velocity in response to a driving force. But APBs also have a thickness which tends to infinity at the critical point [5]. They are therefore also volumes in which there are composition and order parameter gradients. As long as the radii of curvature greatly exceed the thickness, both descriptions are feasible and it becomes important to learn whether or not they are equivalent.

Near the critical point where the interface is thick and the gradients are small it has been shown [5, 7] that the excess free energy due to this inhomogeneous region describes the surface free energy. In this paper we will show that the diffusion that results from the gradients in the inhomogeneous region leads to a translation of the boundary proportional to its mean curvature but *independent of its surface free energy*. We do not explicitly introduce surface free energy, nor for that matter curvature, into the diffusion equation, only the gradients in long-range order parameter η. Within a curved 'surface', the quantity $\nabla^2\eta$ contains quantities that originate from APB curvature and lead to interfacial motion. Because the surface free energy is not a factor in the velocity, we then test the predictions of this theory against the phenomenological theory in systems which have second-order transitions and thus where surface free energy can be varied by several orders of magnitude.

The theoretical treatment that follows was presented earlier [9] in abbreviated form. The experimental data presented here in support of the theory are much more extensive and conclusive than in the earlier paper. We note that a recent paper by Chan [10] treating a more general problem than that considered here obtains theoretical results similar to those we present.

2. DIFFUSE-INTERFACE THEORY AND ANTIPHASE BOUNDARIES

Since we will treat interface motion in terms of a diffusion equation which has been modified to account for gradients in the vicinity of coherent interfaces, it is useful to recall some basic results of diffuse-interface theory [7].

We assume the existence of a function f_o, the free energy per unit volume of a *homogeneous* phase which is a function of the long-range order parameter η. For systems with second-order transitions, all scalar properties including f_o must be even functions of the order parameter, because states with order parameter η' and states with order parameter $-\eta'$ are identical (except for a relative displacement). Below the transition temperature, f_o has the characteristic double-well form indicated in Fig. 1. For such a system the lowest energy state is given by

$$\frac{\partial f_o}{\partial \eta} = 0. \tag{2}$$

Hence for a system with a second-order transition, the equilibrium order parameters are of equal magnitude and opposite sign ($+\eta_e$ and $-\eta_e$ in Fig. 1). The APB is simply the interface between two regions, one with order parameter $+\eta_e$ and the other $-\eta_e$.

Since the interfacial region near an APB comprises a volume in which the order parameter has values intermediate between $+\eta_e$ and $-\eta_e$, surface excess free energy depends on both the details of the function f_o and the spatial variation of the order parameter in the interfacial region. It is customary in discussing excess free energy due to interfaces to in-

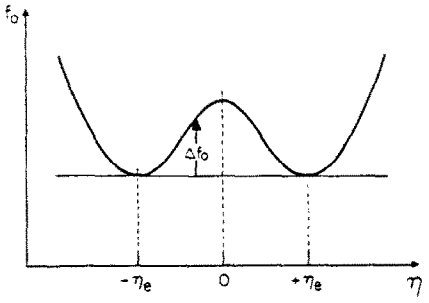

Fig. 1. The free energy per unit volume f_o is an even function of long-range order parameter η. Below the critical temperature, f_o has minima at $\pm\eta_e$. Δf_o is the increase in f_o when η differs from η_e.

troduce the function Δf_o, which is simply the free energy difference between a homogeneous state of arbitrary order parameter and that with $\eta = \pm\eta_e$ (see Fig. 1). For the entire system, the excess free energy due to interfaces is given by

$$\Delta F = \iiint \Delta f \, dV, \tag{3}$$

where the function Δf is given by (7)

$$\Delta f = \Delta f_o + 2\kappa(\nabla\eta)^2 \tag{4}$$

and κ is called the gradient energy coefficient. It can also be shown [8, 11] that the variational derivative $\delta\Delta F/\delta\eta$, which is the change in ΔF when η is varied at a point in a system in which η is varying spatially, is given by

$$\frac{\delta\Delta F}{\delta\eta} = \frac{\partial\Delta f_o}{\partial\eta} - 2\kappa\nabla^2\eta. \tag{5}$$

For planar interfaces at equilibrium, the variational derivative $\delta\Delta F/\delta\eta$ must vanish everywhere, and ΔF will have its minimum value. That is,

$$0 = \frac{\partial\Delta f_o}{\partial\eta} - 2\kappa\frac{\partial^2\eta}{\partial g^2}, \tag{6}$$

where g is distance normal to the interface (along the gradient of η). The first integral of equation (6) gives the expression for an equilibrium planar interface [7]

$$\Delta f_o = \kappa\left(\frac{\partial\eta}{\partial g}\right)^2. \tag{7}$$

Interfaces exist only if κ is positive.

Equation (7) is readily integrated by separation of variables [7] to give the equilibrium profile of a planar interface when the function Δf_o is known, subject to the boundary conditions $\eta = \eta_e$ at $x = \infty$, and $\eta = -\eta_e$ at $x = -\infty$. Since the equation is invariant to translation we choose a particular solution $\eta_p(g)$ such that $\eta_p(0) = 0$. By combining equations (3), (4) and (7) the excess free energy per unit area σ of a planar interface can be expressed

$$\sigma = \int_{-\infty}^{+\infty} 2\kappa\left(\frac{\partial\eta}{\partial g}\right)^2 dg. \tag{8}$$

Also, by using equation (7) to change the integration variable in equation (8),

$$\sigma = \int_{-\eta_e}^{+\eta_e} 2(\kappa\Delta f_o)^{1/2}\, d\eta. \tag{9}$$

For a coherent interface in an unstrained cubic lattice, σ is independent of crystallographic orientation of the interface [7].

Interfacial thickness is easily estimated if the function Δf_o is known. An approximate relationship [7] for the APB thickness l over which $\partial\eta/\partial g$ differs appreciably from zero is easily developed from equation (7) with the result

$$l = 2\eta_e[\kappa/(\Delta f_o)_{max}]^{\frac{1}{2}}, \tag{10}$$

where $(\Delta f_o)_{max}$ is the (local) maximum value of Δf_o which occurs at $\eta = 0$.

For an equilibrium planar APB, the solution to equation (7) for the profile $\eta_p(g)$ is invariant to translation. In the following section, we develop a kinetic theory for diffusion in the interfacial region containing a curved APB. We investigate the implications of the kinetic theory when it is assumed that at some instant a gently curved moving boundary has the profile $\eta_p(g)$.

3. MICROSCOPIC THEORY FOR ANTIPHASE BOUNDARY MOTION

The kinetic equations of continuous ordering reflect the fact that the long-range order parameter η is not a conserved quantity. If the free energy is not at a minimum with respect to a local variation in η, we postulate that there is an immediate change in η given by

$$\frac{\partial\eta}{\partial t} = -\alpha\frac{\delta\Delta F}{\delta\eta}, \tag{11}$$

where α is a positive kinetic coefficient. Substituting equation (5) into (11), we obtain for the time-dependent problem

$$\frac{\partial\eta}{\partial t} = -\alpha\frac{\partial\Delta f_o}{\partial\eta} + M\nabla^2\eta, \tag{12}$$

where $M \equiv 2\alpha\kappa$ has dimensions of a diffusion coefficient (m^2/s). This non-linear equation is similar to the time-dependent Ginsburg–Landau equation in which there is no conservation. It has been discussed by Kawasaki [12] and Metiu *et al.* [13]. Because of the $\partial\Delta f_o/\partial\eta$ term it is non-linear. Its solution will give the evolution of the η field for any initial η distribution. We now investigate the application of equation (12) to the problem of the evolution of an η field in three dimensions which initially describes a curved APB.

It can be shown from a theorem by Wiener (14) that a curved APB obeying equation (12) cannot be in equilibrium; that is, there are no time-independent

solutions. For a spherical APB there is a simple proof which is a corollary to one given previously [15]. We wish to demonstrate that there are no spherically symmetrical solutions to

$$0 = -\frac{1}{\alpha}\frac{\partial \eta}{\partial t} = \frac{\partial \Delta f_o}{\partial \eta} - 2\kappa \frac{d^2\eta}{dg^2} - \frac{4\kappa}{g}\frac{d\eta}{dg}, \quad (13)$$

with the boundary conditions that at $g = 0$, $\eta = \eta_e \neq 0$ and $d\eta/dg = 0$; and at $g = \infty$, $\eta = -\eta_e$ and $d\eta/dg = 0$. If we multiply this equation by $d\eta/dg$ and integrate term by term we obtain respectively for each term

$$\int \frac{\partial \Delta f_o}{\partial \eta}\frac{d\eta}{dg}\,dg = \Delta f_o(-\eta_e) - \Delta f_o(\eta_e) = 0,$$

$$-2\kappa \int \frac{d^2\eta}{dg^2}\frac{d\eta}{dg}\,dg = -\kappa\left(\frac{d\eta}{dg}\right)^2\Bigg]_0^\infty = 0$$

and

$$4\kappa \int \frac{1}{g}\left(\frac{d\eta}{dg}\right)^2 dg > 0.$$

Because the last integral is always positive, there is no solution to equation (13) with these boundary conditions. The only spherically symmetric time independent solution of equation (12) is η = constant, which does not satisfy the boundary conditions below the critical temperature.

We now consider the time dependence of the order parameter within a curved APB as given by equation (12). We assume that the principal radii of curvature of the APB are large compared to the equilibrium thickness and that initially the normal profile of the APB is the same everywhere along the APB. Equation (12) can be rewritten by expanding the term $\nabla^2\eta$. Thus if $\hat{\mathbf{g}}$ is a unit vector normal to the surfaces of constant η, the vector $\nabla\eta$ is given by

$$\nabla\eta = \hat{\mathbf{g}}\frac{\partial \eta}{\partial g}, \quad (14)$$

where $\partial\eta/\partial g$ is the rate of change of η in the direction of $\hat{\mathbf{g}}$. Then we have (see Appendix)

$$\nabla^2\eta = \nabla\cdot\nabla\eta = \frac{\partial^2\eta}{\partial g^2} + \frac{\partial \eta}{\partial g}(\nabla\cdot\hat{\mathbf{g}}) \quad (15)$$

Since the divergence of a unit normal vector to a surface is equal to the negative of the mean curvature $(K_2 + K_2)$ [16], we have for the kinetic equation

$$\frac{\partial \eta}{\partial t} = -\alpha\left\{\frac{\partial \Delta f_o}{\partial \eta} - 2\kappa\left[\frac{\partial^2\eta}{\partial g^2} - (K_1 + K_2)_\eta\frac{\partial \eta}{\partial g}\right]\right\}, \quad (16)$$

where K_1 and K_2 are the principal curvatures of the iso-η surfaces.*

Equation (16) is a general equation governing the time-dependent readjustment of η near a curved APB. We now investigate the motion of a gently curved APB which at some particular time has the profile $\eta_p(g)$ at all normal sections. For this case, equation (7) is valid, and we obtain for the kinetic equation

$$\left(\frac{\partial \eta}{\partial t}\right)_g = -M(K_1 + K_2)\left(\frac{\partial \eta}{\partial g}\right)_t. \quad (17)$$

The velocity $(\partial g/\partial t)$ of a constant η surface in the boundary region is given by

$$\left(\frac{\partial g}{\partial t}\right)_\eta = -\left(\frac{\partial \eta}{\partial t}\right)_g\Big/\left(\frac{\partial \eta}{\partial g}\right)_t. \quad (18)$$

In the limit in which the principal radii of curvature are much greater than the interfacial thickness, the curvatures of the various iso-η surfaces can be considered to be independent of the value of the coordinate g. Therefore all surfaces of constant η at a 'point' in the interface will move with the same velocity V, given by equations (17) and (18) as

$$V = M(K_1 + K_2) \quad (19)$$

and the assumed interfacial profile $\eta_p(g)$ will be preserved in the moving interface.

It is interesting to note at this point that there is a significant difference between equation (19) and the early phenomenological theory which states that the velocity is proportional to surface free energy multiplied by mean curvature, equation (1). In the present development, the surface free energy does not appear in the relationship.

4. MACROSCOPIC THEORY OF DOMAIN GROWTH

Because instantaneous velocities and instantaneous principal curvatures of a point on the interface are difficult to measure, a direct experimental test of equation (19) is difficult to devise and execute. We therefore choose to incorporate our result into a theory of antiphase domain coarsening, in which averages of curvature and velocity are related.

Starting with the linear relation between local velocity and mean curvature, equation (19), and the geometrical relation between the change in area $\delta(dS)$ when an element of area dS of a curved surface moves a distance $V\delta t$ in time δt

$$\delta(dS) = -(V\,\delta t)(dS)(K_1 + K_2), \quad (20)$$

we obtain after rearrangement and substitution of equation (19)

$$\frac{dS}{dt} = -M\int (K_1 + K_2)^2\,dS. \quad (21)$$

in which the time dependence of the experimentally measurable total surface area S appears instead of

* In the present treatment we adopt the convention that the mean curvature is positive when the surface is concave on the side toward which g is directed. Thus a spherical domain has its surface normal directed inward. An opposite convention was used in reference [9], with the result that equations (10) and (11) of that paper have the opposite sign to the analogous equations in this paper.

the local velocities. We define the averaged square mean curvature K_m^2

$$K_m^2 = \langle (K_1 + K_2)^2 \rangle = \frac{1}{S}\int (K_1 + K_2)^2 \, dS. \quad (22)$$

The surface area in a unit volume of specimen, S_v, then obeys the relation

$$\frac{dS_v}{dt} = -MK_m^2 S_v. \quad (23)$$

We now consider superlattices having only two antiphase domains. The B2 (CsCl) structure is an example. If dislocations in the crystal are ignored, each domain is multiply connected [17]. As the domain structure coarsens, interconnections are broken, and both K_m^2 and S_v decrease. If we assume that during coarsening the statistical measures of the structure change only as a result of the length scale changes, then both S_v^2 and K_m^2 will be proportional to the reciprocal of the square of this length scale. Hence

$$K_m^2 = \phi S_v^2, \quad (23)$$

where statistical similarity of the structure during coarsening implies that ϕ is a constant. Substituting equation (23) into (22) and integrating, we obtain

$$[S_v(t)]^{-2} - [S_v(0)]^{-2} = 2\phi Mt, \quad (24)$$

where $S_v(0)$ is the initial value of S_v, and $S_v(t)$ is the value at time t.

5. DISSIPATION IN THE MICROSCOPIC THEORY

As has been noted in the introduction, it is customary to view surface excess properties (like free energy) on a per unit area basis, thus treating the interface as a geometrical surface. In such a picture, interfacial motion lowers the free energy of the system by decreasing the surface area of the interfaces. Thus the *dissipation*, or rate of free energy decrease for the system due to interfacial motion is given by

$$\frac{\partial F}{\partial t} = \sigma \frac{dS}{dt}. \quad (25)$$

In our treatment we did not implicitly define the surface tension σ and the only irreversible process was diffusional. Since the calculated velocity does not depend on σ it becomes important to check whether the dissipation due to the diffusion that leads to interface motion is equal to that given by equation (25). The dissipation is given by a volume integral

$$\frac{\partial F}{\partial t} = \iiint \frac{\delta \Delta F}{\delta \eta} \cdot \frac{\partial \eta}{\partial t} \, dv. \quad (26)$$

It is interesting to note that the integrand $\delta \Delta F/\delta \eta \cdot \partial \eta/\partial t$ which is $\partial \Delta f/\partial t$ in a unit volume is not the dissipation because there can be a flux of free energy. A moving APB, for instance, will 'carry' excess free energy along with it and in so doing some elements of volume will lose and some will gain free energy.

For the case of 'almost planar' APBs, whose radii of curvature greatly exceed the interfacial thickness, equation (17) is valid. Making use of equations (5), (15) and (17), equation (26) gives for the dissipation

$$\frac{\partial F}{\partial t} = -\iiint 2\kappa \left(\frac{\partial \eta}{\partial g}\right)^2 \cdot V(K_1 + K_2) \, dv. \quad (27)$$

The volume of integration in equation (27) can be separated into two parts: one for the antiphase domain interiors, and one for volumes which completely contain the inhomogeneous regions where there are interfaces. The first part does not contribute to the dissipation, as $\partial \eta/\partial g$ is zero everywhere within the domain interiors. An element of volume in the second part can be expressed as

$$dv = dg \cdot dS \quad (28)$$

where dS is an element of surface area and g, as before, is the distance along the gradient (see Fig. 2). Since the interface is thin relative to its radii of curvatures dS and K_1 and K_2 are independent of g, and the volume integral can be expressed

$$\frac{\partial F}{\partial t} = -2\int_{-\delta}^{\delta} \kappa \left(\frac{\partial \eta}{\partial g}\right)^2 dg \cdot \iint V(K_1 + K_2) \, dS. \quad (29)$$

where the integration limit δ is sufficiently large to extend into regions on both sides of the interface where $\partial \eta/\partial g$ vanishes. From equation (8), the first integral in equation (29) is seen to be equal to σ, the surface free energy. Comparing the second integrand with equation (21), we have

$$\iint V(K_1 + K_2) \, dS = -\frac{dS}{dt} \quad (30)$$

and hence equation (29) becomes

$$\frac{\partial F}{\partial t} = \sigma \frac{dS}{dt}. \quad \text{Q.E.D.}$$

The microscopic theory, in which interfacial motion as derived from a diffusion equation as not being proportional to σ gives the correct expression for dissipation of surface free energy.

6. SELECTION OF EXPERIMENTAL SYSTEM

Equation (19) is the central result of the theory for APB motion which we wish to test experimentally. We have chosen to test the theory by studying the coarsening of antiphase domain structures in systems that have second-order transitions. Two critical aspects of the theory can be tested: first, that equation (24) is obeyed for domain coarsening at a fixed temperature; and second, that over a range of temperatures where σ can be varied appreciably, the quantity

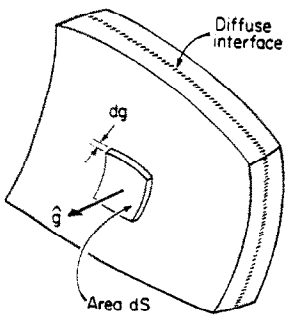

Fig. 2. An element of 'surface volume' in a sheet of finite thickness containing a diffuse interface. The volume element dv is equal to $d\mathbf{g}\cdot d\mathbf{S}$ if the thickness of the inhomogeneous region is small relative to the radii of curvature.

ϕM in equation (24) does *not* have the temperature dependence of σ. The surface free energy can be varied appreciably in any system in which the order–disorder transition is second order. Examples are Cu–Zn, Fe–Al and Fe–Si.

A portion of the Fe–Al coherent phase diagram [18, 19, 20, 21] is reproduced in Fig. 3. The phases α, FeAl, and Fe_3Al possess the A2(b.c.c.), B2 and DO_3 structures†, respectively. The FeAl phase is stable far from stoichiometry; the excess iron atoms are accommodated substitutionally on the aluminum sublattice. The $\alpha \rightarrow$ FeAl phase transition is second-order along a line in the phase diagram which terminates at a tricritical point [22] at about 23% Al‡ and 890 K; below this temperature the phase change is first-order. The FeAl $\rightarrow$ Fe_3Al transition is second-order until it terminates at a three-phase invariant.

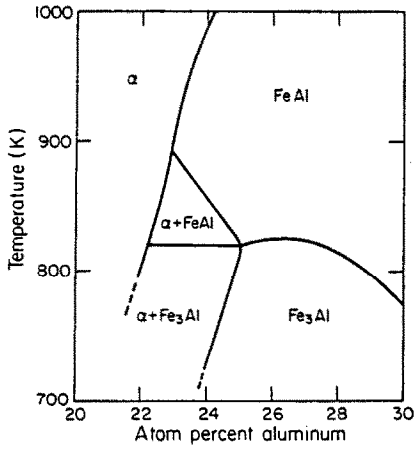

Fig. 3. The coherent phase diagram for the Fe–Al system [20, 21].

† Strukturbericht notation.

‡ All compositions reported in this paper are atomic percent.

§ As noted earlier, Fe_3Al specimens received an intermediate FeAl ordering treatment which was carried out at about 900 K for at least 1 h.

Atomic arrangements and possible APB displacement vectors in the B2 and DO_3 structures are shown schematically in Fig. 4. In the B2 structure, there is only one kind of APB, having a $\frac{1}{2}a_o\langle 111\rangle$ displacement vector. In the DO_3 structure two types of displacement vectors produce APBs, $\frac{1}{2}a_o'\langle 111\rangle$ and $\frac{1}{2}a_o'\langle 100\rangle$. The two types in the DO_3 structure can be distinguished by dark-field electron microscopy [23]. We chose to perform an electron microscope study of domain coarsening in an Fe–23%Al alloy with FeAl order, and in an Fe–24%Al alloy we studied domain growth in both the FeAl and Fe_3Al phases. In the Fe_3Al phase, we studied growth of the $\frac{1}{2}a_o'\langle 100\rangle$ antiphase domains only. This was accomplished by producing very large $\frac{1}{2}a_o\langle 111\rangle$ domains in an FeAl ordering treatment prior to heat treatment in the Fe_3Al region of the phase diagram. A fine-scale Fe_3Al domain structure consisting of only two domains, distinguished by a $\frac{1}{2}a_o'\langle 100\rangle$ displacement, forms within each FeAl domain. This finer domain structure is topologically very similar to that in the FeAl phase.

An extensive domain coarsening study in an Fe–Co alloy with small vanadium additions has already been made by English [17]. Domain coarsening in an Fe–49%Co–2%V alloy with B2 order was studied by X-ray diffraction. We have chosen to re-examine these data in the light of our new theory, although there are no data close to the disordering transition.

7. EXPERIMENTAL TECHNIQUES

The Fe–Al alloys used in this study were the same ones used in an earlier study [24]. Their nominal compositions are Fe–23.0%Al and Fe–24.0%Al. The following heat treatment sequence was used: homogenization treatment at 1050 K or above in an inert atmosphere, followed by a brine quench; and a single ordering and antiphase domain growth treatment§ at a temperature below the critical temperature for ordering, followed by a brine quench. For the homogenization treatment the material was in rod form, having 3 mm dia. For the ordering and domain growth treatment, discs 3 mm in dia. and 0.2 mm thick were wrapped in stainless steel foil and heat treated in molten salt or lead. The temperature of the molten bath was typically maintained constant to within 1 K during heat treatments. Electron microscope samples were prepared by electropolishing the 3 mm discs using techniques described earlier [24].

Heat treatment times used for the single ordering and domain growth heat treatments were very much greater than the time necessary for complete ordering: in this way the term $S_v^{-2}(0)$ in equation (24) was made negligibly small. The maximum allowable heat treatment times are determined by the dislocation density in the sample, because APBs terminate at dislocations having a Burger's vector which is not a translation vector of the superlattice. Domain growth stopped when domain size became of the order of the disloca-

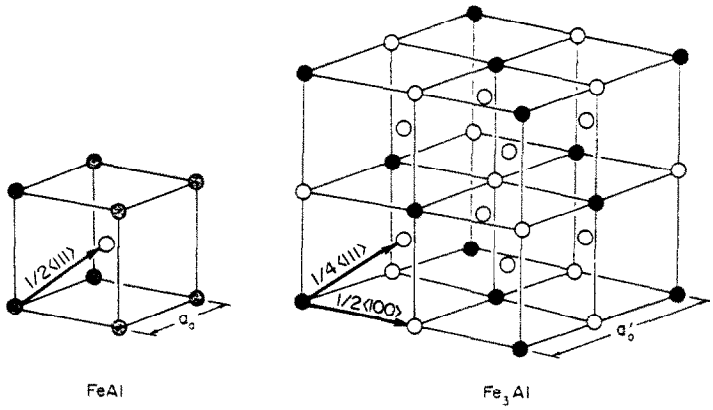

Fig. 4. Atomic arrangements and possible superlattice displacement vectors for the ordered phases FeAl and Fe_3Al. Both phases are derivatives of b.c.c.

tion spacing. Thus for measurements of the kinetics of antiphase domain coarsening, we endeavored to have the mean linear intercept for APBs be considerably smaller than the mean distance between dislocations, or other factors that interfere with the statistical similarity assumed in equation (23). The Fe_3Al domain coarsening heat treatments were terminated before the Fe_3Al domain size reached the prior FeAl domain size.

Measurements of APB surface area per unit volume were made on transmission electron micrographs using standard quantitative metallographic procedures [25, 26]. For each data point a minimum of 38 intersections of APBs with the test circle were counted, making the sampling error for S_v less than 10%. Because micrographs were taken from areas of finite specimen thickness, a first-order correction was applied in cases where a test line was tangent to (thus overlapping the projected image width) an APB in a micrograph. In such a case one intersection of the test line with the APB was counted.

An analysis of English's data for domain growth in the Fe–Co–2V alloy requires that a value for $S_v^{-2}(0)$ in equation (24) be taken into account because the maximum domain sizes achieved in these experiments were so small. The following method was used: English reported domain sizes achieved after different heat treatment times for several temperatures, and also the time for the samples to reach 90% of the equilibrium value of the order parameter at each temperature. Heat treatment times which were longer than this were considered to produce 'fully' ordered specimens, and these data were used for the present domain growth analysis. The longest heat treatments at 898, 838, 823 and 798 K were discarded because it appeared that there might have been systematic errors in the domain size measurements when the domain sizes were large. A linear regression analysis of D^2 vs t (where D is the domain size and t is the heat treatment time) for the remaining data at each temperature was made. From the slope, a 'best' value of $(S_v^2 t)^{-1}$ at each temperature was computed.

8. EXPERIMENTAL RESULTS AND DISCUSSION

8.1 *Time dependence*

The time dependence of antiphase domain coarsening at constant temperature has been extensively investigated by others [27–33]. We expect a linear relationship between time and the square of the domain size during the period where equations (1) or (19), and equation (23) are valid. Implicit in (1) and (19) is an absence of anisotropy, which obviously eliminates domain coarsening studies in $L1_2$ structures such as Cu_3Au [30, 31] and Ni_3Fe [32] from consideration. Equation (23) eliminates the initial time period during which asymptotic domain shape implied by equation (23) is being established. It also eliminates the long time period where the domain size is approaching the grain or specimen size or the dislocation spacing, whichever is smallest.

Since this paper is concerned with the distinction between equations (1) and (19), the time dependence is not a central issue. Nevertheless it is worthwhile to point out that the expected time dependence was found both by English [17] as shown by his Fig. 2, and by us in a single check (Table 1, Fe–24%Al 898 K). The time dependence implies that $S_v^2 t$ is a constant in time, but not in temperature. It is equal to $2\phi M$ if equation (19) is valid, or $2\phi\mu\sigma$ if equation (1) is valid. These should differ greatly in their temperature dependence near the critical point where σ tends to zero. We note that several workers have studied isothermal domain growth in the Fe_3Al phase experimentally at temperatures below 694 K, [27, 28, 29] where the ordering times are rather long. Careful scrutiny of the accompanying data concerning the kinetics of the ordering reaction [27, 29] show that most of the reported data on domain size are for heat treatment times shorter than or approximately equal to that required for complete ordering. For this reason, we do not make use of these results in testing our theory.

Table 1. Antiphase domain growth in Fe–Al and Fe–Co–2V alloys

T (K)	t (s)	$\{S_v^2 t\}^{-1}$ (m²/s)
Fe–24%Al, FeAl order		
990	300	1.1×10^{-17}
987	300	1.5×10^{-15}
983	300	1.5×10^{-15}
965	300	1.1×10^{-15}
953	300	1.1×10^{-15}
931	600	5.6×10^{-16}
904	1200	2.2×10^{-16}
898	3600	1.1×10^{-16}
898	360	1.1×10^{-16}
871	3600	3.9×10^{-17}
Fe–23%Al, FeAl order		
908	1200	disordered
904	1200	1.3×10^{-16}
895	1440	6.9×10^{-17}
889	1200	5.4×10^{-17}
884	1200	1.6×10^{-17}
883 ± 4	6000	3.6×10^{-18}
Fe–24%Al, Fe_3Al order		
768.5	68,400	1.0×10^{-19}
758	86,400	7.1×10^{-20}
748	86,400	6.4×10^{-20}
720	1.64×10^6	5.8×10^{-20}
Fe–26.5, Fe_3Al order [40]		
823	1.01×10^5	2×10^{-18}
Fe–Co–2V, FeAl order [17]		
898	60 – 240	6.9×10^{-19}
853	120 – 950	1.0×10^{-19}
838	240 – 3200	4.3×10^{-20}
823	880 – 5500	1.2×10^{-20}
798	910 – 14,800	3.6×10^{-21}

8.2 *Temperature dependence*

Our data for domain coarsening in Fe–Al alloys is listed in Table 1. In Fig. 5 we show $S_v^2 t$ vs temperature for these data on an Arrhenius plot. On such a plot the deviations from a straight line demonstrate the presence of temperature dependent factors or terms other than a simple $\exp(-Q/RT)$.

It is important to establish whether the temperature dependence of the data in Fig. 5 are consistent with equations (1) or (19). The behavior of σ near the critical temperature is known to vary as $[(T_c - T)/T_c]^{\gamma}$, where γ is approximately 1.3 [34]. The other dominant temperatue dependence in M or μ will be due to the activation energy of atomic motion and will be of the form $\exp(-Q/RT)$. Functions of the form $[(T_c - T)/T_c]^{\gamma}\exp(-Q/RT)$, when plotted on Fig. 5, will at low temperatures asymptotically approach the slope of $-Q/R$ but with $\gamma > 0$ will reach a maximum and change slope at approximately $(T_c - T)/T_c = \gamma RT_c/Q$. Near T_c the slope will tend to ∞. If the exponent γ were negative there would be no maximum and the slope would tend to $-\infty$, with the marked deviation from the Arrhenius plot beginning at $(T_c - T)/T_c = -\gamma RT_c/Q$.

The principal temperature dependence of M or μ should mirror that of diffusion within the APB, which is a region of varying degrees of order. Even diffusion in homogeneously ordered alloys has an apparently variable activation energy due to temperature dependences of thermodynamic factors and correlation factors [35, 36]. In addition it is known that the factor K in M should have a weak divergence close to T_c proportional to $[(T_c - T)/T_c]^{-0.02}$ where the exponent is equal to the product of the exponents for the pair correlation function and the correlation length [37]. Current best theoretical estimates from a three-dimensional Ising model are 0.031 and 0.63, respectively [38].

In addition, if μ is inversely proportional to the thickness of the APB as has been suggested for some kinds of surfaces [2], an additional factor of $[(T_c - T)/T]^{0.63}$ would appear in equation (1) raising the temperature exponent to almost 2.

We now turn to the individual systems for which we have listed domain coarsening data in Table 1.

Domain growth in Fe–24%Al *with* FeAl *order.* These data span the temperature interval between 990 and 871 K. The domain structure produced at 990 K is indicative of ordering during the quench; thus the critical temperature for our 24% alloy is bracketed between 987 and 990 K. This alloy is two-phase below about 860 K (see Fig. 3). The semi-logarithmic plot of the data in Fig. 5 shows that to an excellent approximation $(S_v^2 t)^{-1}$ is an Arrhenius function of temperature.

A regression analysis of these data was performed to determine 90% confidence intervals for the appar-

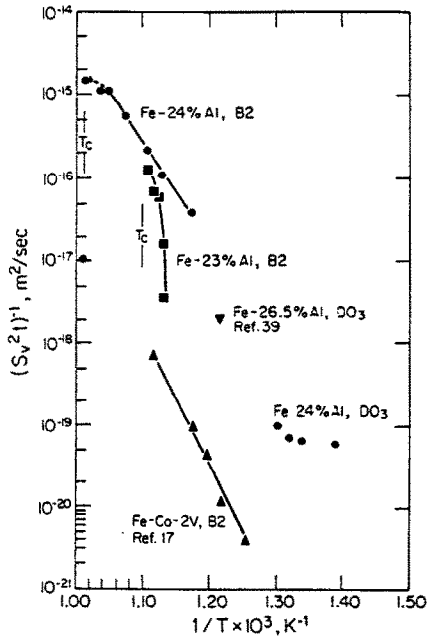

Fig. 5. Graph of experimental data for antiphase domain growth in Fe–Al and Fe–Co–2V alloys. S_v is the APB surface area per unit volume, t is the ordering time and T is the ordering temperature.

ent activation energy Q for the process. The resulting interval was

$$200{,}000 \text{ J/mol} \leq Q \leq 270{,}000 \text{ J/mol}.$$

If $\{S_v^2 t\}^{-1}$ was proportional to σ multiplied by an Arrhenius function having an activation energy of 235,000 J/mol, then the plot of the data in Fig. 5 would go through a maximum at about 45 K below the critical temperature. Clearly, then, the data do not display the temperature dependence of σ.

Domain growth in Fe–23%Al *with* FeAl *order.* These data span the temperature range from 908 to 884 K. The critical temperature for this alloy is found experimentally to lie between 904 and 908 K. Below about 890 K, electron micrographs show the microstructure to be two-phase. The APBs in these two-phase specimens are coated with a distinct layer of the disordered phase which is of the order of 10 nm in thickness.

Antiphase domain growth in FeAl ordered Fe–23%Al is of interest because this composition is close to the tricritical point in the phase diagram, where the line of higher-order transitions for the $\alpha \rightarrow$ FeAl reaction intersects the two-phase α + FeAl region. At the tricritical point, $\partial^2 f_v / \partial c^2$ vanishes in the ordered phase [21], where c is the composition. Therefore, fluctuations in composition in FeAl-ordered specimens will be large in the vicinity of the tricritical point. Adsorption of excess iron atoms on APBs is also likely to occur near the tricritical point in the FeAl region of the phase diagram [39]. Since our theory only accounts for variations in long-range order parameter, it is of interest to see how domain growth in the 23% Al alloy compares with that in the 24% alloy at the same temperature. The 24% alloy is 80 K further from its critical temperature. It is more highly ordered and its value of σ is at least an order of magnitude greater. In Fig. 5 it is seen that in the temperature range between 895 and 904 K, domain growth occurs nearly as rapidly in the 23%Al alloy as in the 24%Al alloy. Electron micrographs of the domain structures in the Fe–23%Al alloy reveal quenched-in fluctuations in degree of long-range order that are absent in Fe–24%Al alloys heat treated at similar temperatures, as shown in Fig. 6. In addition, the APBs themselves are very ragged in the former alloy, and smoothly curved in the latter. It is interesting that even with these different structures and σ's domain growth in these two alloys occurs with comparable speeds, as would be expected from equation (19).

Domain growth in Fe–23%Al specimens which are two-phase α + FeAl is slowed considerably relative to single-phase FeAl specimens. Since the α phase coats the APBs and differs in composition from the ordered phase, this is not surprising. The apparent activation energy for domain coarsening in the two-phase specimens, as indicated by the slope of the curve for the 23%Al alloy in Fig. 5, is much greater than for the single-phase Fe–24% alloy.

Domain growth in Fe–24%Al *with* Fe_3Al *order.* These data span the temperature range between 768 and 720 K. Only at the lowest temperature is the specimen clearly single-phase Fe_3Al. At the other temperatures studied, contrast in dark-field electron micrographs indicates that there is a layer of disor-

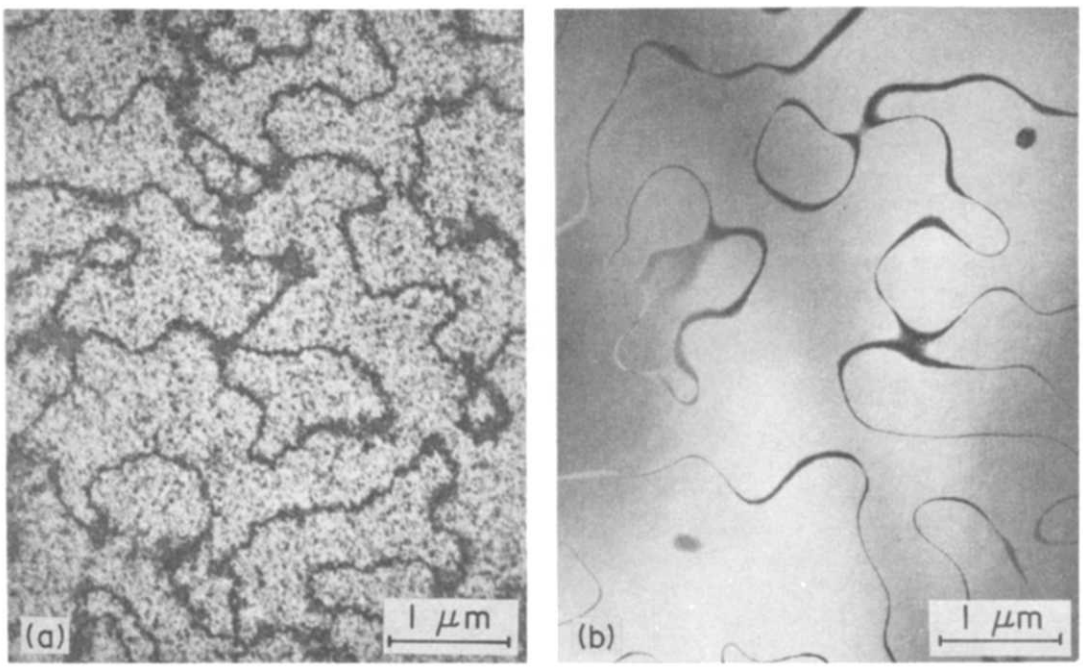

Fig. 6. Dark-field electron micrographs showing APB structures in (a) Fe–23%Al and (b) Fe–24%Al after identical ordering treatments at 904 K for 1200 s. The 23% alloy is within 4 K of its critical temperature and shows quenched-in critical fluctuations.

dered phase at APBs. At 758 and 768 K this layer is several nm thick. The data point at 720 K lies roughly along the extrapolation of the curve for FeAl-ordered Fe–24%Al alloys in Fig. 5. The value of $\{S_\sigma^2 t\}^{-1}$ achieved in the two-phase $\alpha + Fe_3Al$ specimens arrears to be relatively insensitive to the heat treatment temperature.

Domain growth near T_c *in* Fe–26.5%Al *with* Fe_3Al *order.* In a unique experiment, Swann *et al.* [40] studied a specimen held for 28 h in a temperature gradient which included T_c for their 26.5% Al alloy. From an estimate of the domain size in their published micrographs, the data point in Table 1 was determined. Their micrographs cover a temperature range of 7 K, over which σ should be varied by more than a factor of twenty. Even to within a fraction of 1 K of the critical temperature, there was no noticeable trend in domain size with temperature.

Domain growth in Fe–Co–2V *with* FeAl *order.* The temperature dependence of English's data for Fe–Co–2V is evident from Fig. 5. The data display the Arrhenius behavior found in the Fe–24% Al alloy with FeAl order. The reported activation energy [17] in Fe–Co–2V, 290,000 J/mol, is somewhat higher than that for the Fe–Al alloy. The curve for Fe–Co–2V lies approximately two orders of magnitude below the curve for Fe–24%Al.

On the basis of these individual experimental results we conclude that APB velocity is not governed by equation (1). Whether it is quantitatively governed by equation (19) must await an experimental measurement of the geometrical factor ϕ and the kinetic factor α which, as defined in equation (11), is a phenomenological parameter which can be measured in diffusion or ordering experiments that are completely independent of any domain wall problems.

9. CRITIQUE

As our new theory now stands, its applicability to antiphase domain coarsening in real systems is limited primarily by three constraints. First, the new theory is strictly valid only for phases in which the order–disorder reaction is higher than first-order. We note that Chan [10] considered interfacial motion in systems which did not have symmetric (about $\eta = 0$) free energy functions, but the application of Chan's results to APB motion in such systems has not been made. Second, the new theory makes use of diffuse-interface theory in a way that makes the results valid only for systems in which the APB energy is isotropic. Third, when more than one kind of APB is possible, as in Cu_3Au where both 'conservative' and non-conservative types can exist, equation (23) implies that the proportion of each type be constant during domain coarsening. In Au_3Cu there is evidence that this latter constraint is not true [41].

The phenomenological statement in equation (1) linearly relates interfacial velocity to driving force. Non-linear relations have also been proposed [3, 42]. As the beginning point for our theoretical treatment of the motion of a curved APB, we have chosen a different phenomenological expression—a linear relation between the rate or order change and the driving force for ordering, equation (11). Our resulting equation for interfacial velocity, equation (19), is not a relationship of velocity to driving force, since driving force must include σ. Nonetheless, it is gratifying to note that the diffusional dissipation of free energy of an APB obeying equation (19) is exactly equal to the available driving force.

This paper concludes that equation (1) is not universally valid. There are, however, clearly cases where it is valid. In the case of a curved soap film, the pressure difference in the gases leads to gas transpiration rates proportional to the driving force and, incidentally, like Turnbull's theory [2] inversely proportional to the thickness. The soap film theory, like the theory of Li for the motion of a cylindrical tilt boundary [41] and the theory of the present paper, is derived from more basic phenomenological theories which in turn can each be tested in independent experiments. In Li's case, he is invoking the force–velocity relation on the individual dislocations; in our case we invoke ordering kinetics in a region that has not achieved equilibrium order. At present we seem to have theories that are linearly and non-linearly dependent in curvature, that are independent, linearly dependent and non-linearly dependent on σ, and that are independent or linearly dependent on the reciprocal of the thickness. If there is a universal law relating velocity to curvature, it does not seem apparent at this time.

Acknowledgements—We are grateful to the National Science Foundation for support of the portion of the research performed at MIT. Robert M. Allen of MIT performed a statistical analysis of the data. Helpful discussions with Professor James Litster of the Physics Department at MIT concerning the critical behavior of the gradient energy coefficient are gratefully acknowledged.

REFERENCES

1. R. Smoluchowski, *Phys. Rev.* **83**, 69 (1951).
2. D. Turnbull, *Trans. AIME* **191**, 661 (1951).
3. B. Sundquist, *Metall. Trans.* **4**, 1919 (1973).
4. J. W. Cahn, *Acta metall.* **10**, 789 (1962).
5. R. Kikuchi, *J. Phys. Chem. Solids* **27**, 1305 (1966).
6. J. S. Langer and R. Sekerka, *Acta metall.* **23**, 1225 (1975).
7. J. W. Cahn and J. Hilliard, *J. chem. Phys.* **28**, 258 (1958).
8. J. W. Cahn, *Acta metall.* **9**, 795 (1961).
9. J. W. Cahn and S. M. Allen, *J. de Physique, Colloque* C-7, 54 (1977).
10. S.-K. Chan, *J. chem. Phys.* **67**, 5755 (1977).
11. J. W. Cahn and J. E. Hilliard, *Acta metall.* **19**, 151 (1971).
12. K. Kawasaki, *Prog. theor. Phys.* **57**, 410 (1977).
13. H. Metiu, H. Kitahari and J. Ross, *J. chem. Phys.* **64**, 292 (1976).
14. R. Courant and D. Hilbert, *Methods of Mathematical Physics*, Vol. 2, p. 305. Interscience, New York (1962).
15. J. W. Cahn and J. Hilliard, *J. chem. Phys.* **31**, 688 (1959).

16. C. Weatherburn, *Differential Geometry of Three Dimensions*, p. 225. Cambridge Univ. Press, Cambridge (1927).
17. A. English, *Trans. AIME* **236**, 14 (1966).
18. P. R. Swann, W. R. Duff and R. M. Fisher, *Trans. AIME* **245**, 851 (1969).
19. H. Okamoto and P. A. Beck, *Metall. Trans.* **2**, 569 (1971).
20. P. R. Swann, W. R. Duff and R. M. Fisher, *Metall. Trans.* **3**, 409 (1972).
21. S. M. Allen and J. W. Cahn, *Acta metall.* **23**, 1017 (1975).
22. R. B. Griffiths, *J. chem. Phys.* **60**, 195 (1974).
23. M. J. Marcinkowski and N. Brown, *J. appl. Phys.* **33**, 537 (1962).
24. S. M. Allen and J. W. Cahn, *Acta metall.* **24**, 425 (1976).
25. C. S. Smith and L. Guttman, *Trans. A.I.M.E.* **197**, 81 (1953).
26. J. E. Hilliard, Applications of quantitative metallography in recrystallization studies, in *Recrystallization, Grain Growth and Textures*, p. 267. Metals Park, American Society for Metals (1965).
27. K. Oki, M. Hasaka and T. Eguchi, *Trans. Jap. Inst. Metals* **14**, 8 (1973).
28. L. Rimlinger, *C.r. Acad. Sci. Paris* **272**(C), 22 (1971).
29. H. Sagane, A. Yamamura, K. Oki and T. Eguchi, *J. Jap. Inst. Metals* **39**, 1076 (1975).
30. M. Sakai and D. E. Mikkola, *Metall. Trans.* **2**, 1635 (1971).
31. C. L. Rase and D. E. Mikkola, *Metall. Trans.* **6A**, 2267 (1975).
32. F. Bley and M. Fayard, *Acta metall.* **24**, 575 (1976).
33. S. M. L. Sastry and H. Lipsitt, *Metall. Trans.* **8**(A), 1543 (1977).
34. H. E. Stanley, *Introduction to Phase Transitions and Critical Phenomena*, p. 47. Oxford University Press, Oxford (1971).
35. A. Kuper, D. Lazarus, J. R. Manning and C. T. Tomizuka, *Phys. Rev.* **104**, 1536 (1956).
36. J. E. Hilliard, in appendix to paper by J. E. Reynolds, B. L. Averbach and M. Cohen, *Acta metall.* **5**, 29 (1957).
37. J. Litster, private communication.
38. J. C. LeGuillou and J. Zinn-Justin, *Phys. Rev. Lett.* **39**, 95 (1977).
39. B. Widom, *Phys. Rev. Lett.* **34**, 999 (1975).
40. P. R. Swann, W. R. Duff and R. M. Fisher, *Phys. Status Solidi* **37**, 577 (1970).
41. P. M. Bronsveld and S. Radelaar, *J. phys. Soc. Japan* **38**, 1336 (1975).
42. J. C. M. Li, *Trans. A.I.M.E.* **245**, 1591 (1969).
43. G. Arfken, *Mathematical Methods for Physicists*, pp. 65–69. Academic Press, New York (1968).

APPENDIX

Divergence of a Gradient Vector in Orthogonal Curvilinear Coordinates

A general expression for the divergence of a gradient vector to a scalar field $\eta(q_1, q_2, q_3)$ in orthogonal curvilinear coordinates is given [43]. Consider the η field to be comprised of constant η surfaces. An orthogonal curvilinear coordinate system may be defined such that one coordinate q_1 is everywhere normal to the iso-η surfaces. At any point the other two axes q_2 and q_3 are necessarily tangent to an iso-η surface. Then we have

$$\nabla^2\eta = \frac{1}{h_1h_2h_3}\left[\frac{\partial}{\partial q_1}\left(\frac{h_2h_3}{h_1}\frac{\partial\eta}{\partial q_1}\right)\right], \tag{A-1}$$

where (h_1, h_2, h_3) is the metric which relates differential distances in the coordinate system to differential increments of the coordinate axes. In particular, if the distance along the axis q_1 is measured by a parameter g, then

$$dg = h_1\,dq_1 \tag{A-2}$$

and equation (A-1) can be expressed

$$\nabla^2\eta = \frac{1}{h_2h_3}\frac{\partial}{\partial g}\left(h_2h_3\frac{\partial\eta}{\partial g}\right). \tag{A-3}$$

Expanding equation (A-3) and making use of (A-2) gives the result

$$\nabla^2\eta = \frac{\partial^2\eta}{\partial g^2} + \frac{\partial\eta}{\partial g}\cdot\frac{1}{h_1h_2h_3}\left[\frac{\partial}{\partial q_1}(h_2h_3)\right]. \tag{A-4}$$

In the same notation the divergence of a unit normal $\hat{\mathbf{g}}$ to an iso-η surface is given by [43]

$$\nabla\cdot\hat{\mathbf{g}} = \frac{1}{h_1h_2h_3}\left[\frac{\partial}{\partial q_1}(h_2h_3)\right]. \tag{A-5}$$

Equation (15) thus follows from equations (A-4) and (A-5).